

Source properties of the 1998 July 17 Papua New Guinea tsunami based on tide gauge records

Mohammad Heidarzadeh and Kenji Satake

Earthquake Research Institute, The University of Tokyo, Tokyo, Japan. E-mail: mheidar@eri.u-tokyo.ac.jp

Accepted 2015 March 30. Received 2015 February 5

SUMMARY

We analysed four newly retrieved tide gauge records of the 1998 July 17 Papua New Guinea (PNG) tsunami to study statistical and spectral properties of this tsunami. The four tide gauge records were from Lombrum (PNG), Rabaul (PNG), Malakal Island (Palau) and Yap Island (State of Yap) stations located 600–1450 km from the source. The tsunami registered a maximum trough-to-crest wave height of 3–9 cm at these gauges. Spectral analysis showed two dominant peaks at period bands of 2–4 and 6–20 min with a clear separation at the period of ~5 min. We interpreted these peak periods as belonging to the landslide and earthquake sources of the PNG tsunami, respectively. Analysis of the tsunami waveforms revealed 12–17 min delay in landslide generation compared to the origin time of the main shock. Numerical simulations including this delay fairly reproduced the observed tide gauge records. This is the first direct evidence of the delayed landslide source of the 1998 PNG tsunami which was previously indirectly estimated from acoustic T-phase records.

Key words: Fourier analysis; Wavelet transform; Tsunamis; Earthquake source observations; Submarine landslides; Pacific Ocean; Papua New Guinea.

1 INTRODUCTION

The 1998 July 17 Papua New Guinea (PNG) landslide tsunami, triggered by a moderate M_w 7.0 earthquake off PNG (Fig. 1), has been an important tsunami event since it was the largest recorded landslide tsunami of modern times with a death toll of more than 2100 (Tappin *et al.* 2001; Synolakis *et al.* 2002). Being a shake up call for potential large tsunami hazards from submarine landslide tsunamis which was not well recognized before this tsunami, the PNG event was soon at the centre of attention in the tsunami community and was studied by numerous authors (Matsuyama *et al.* 1999; Okal 1999; Tanioka 1999; Tappin *et al.* 1999, 2001; Geist 2000; Heinrich *et al.* 2000, 2001; McSaveney *et al.* 2000; Synolakis *et al.* 2002; Lynett *et al.* 2003; Satake & Tanioka 2003; Watts *et al.* 2003; Okal & Synolakis 2004). These studies were mostly concentrated on the characterization of the tsunami source using coastal runup heights from field surveys, geological mapping of the seafloor and numerical modelling of hypothetical landslide source scenarios because the earthquake-generated seafloor deformation was far inadequate to generate large runup heights of ~15 m.

While most of the previous studies were successful in reproducing the observed runup heights using their proposed landslide sources, the sea level records of the tsunami were not used to further validate the tsunami source or to characterize the tsunami properties. Among the previous studies, two of them (i.e. Tanioka 1999; Satake & Tanioka 2003) reported far-field tsunami waveforms along the coast of Japan. Here, we present for the first time four tsunami waveforms of the 1998 July 17 PNG tsunami in Lombrum (PNG),

Rabaul (PNG), Malakal Island (Palau) and Yap Island (State of Yap) which are located at the distances of ~600, ~1120, ~1420 and ~1450 km from the source, respectively (Fig. 1). These tsunami waveforms help to: (1) provide new insights into the statistical and spectral properties of the 1998 PNG tsunami, (2) study the contribution of landslide and earthquake sources to the 1998 PNG tsunami and (3) propose a combined source including both earthquake and landslide sources for this important tsunami.

2 A SHORT REVIEW OF THE 1998 PNG TSUNAMI

At 08:49 GMT on 1998 July 17, an M_w 7.0 earthquake (Kikuchi *et al.* 1999) occurred off north of PNG whose epicentre was inland according to the United States Geological Survey (USGS; Fig. 1). However, the aftershocks were distributed at offshore area (Fig. 1b) as previously reported by Kikuchi *et al.* (1999) and McSaveney *et al.* (2000). Although there have been disagreements on the fault parameters of the earthquake, most of the published studies reported a maximum seismic slip of ~1–2 m which could produce a maximum coastal runup of ~1–2 m (Synolakis *et al.* 2002; Satake & Tanioka 2003; Watts *et al.* 2003). To reproduce the observed runup heights of ~15 m, a landslide/slump source was proposed (the colour map in Fig. 1b and the 3-D plot in Fig. 1c; Heinrich *et al.* 2000; Synolakis *et al.* 2002; Satake & Tanioka 2003; Watts *et al.* 2003) which was supported by the bathymetric survey of the offshore region (Tappin *et al.* 2001).

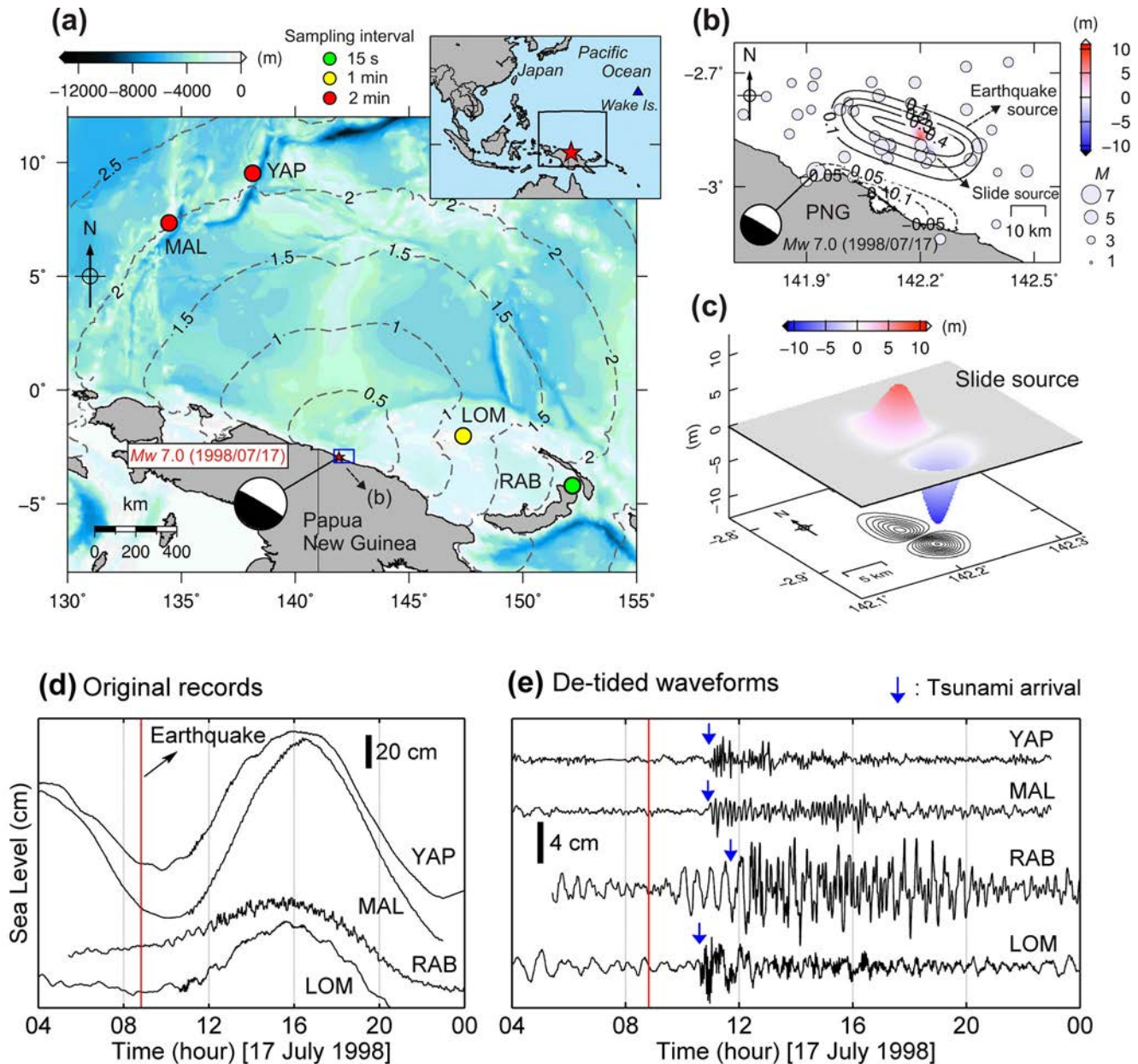


Figure 1. The 1998 July 17 Papua New Guinea earthquake and tsunami. (a) The locations of the epicentre (red asterisks) from US Geological Survey (USGS) with focal mechanism from Kikuchi *et al.* (1999) and four tide gauges used in this study. LOM, RAB, MAL and YAP represent Lombrum, Rabaul, Malakal Island and Yap Island, respectively. Dashed contours are tsunami travel times in hours. (b) The previously proposed source models for the July 1998 PNG tsunami according to Synolakis *et al.* (2002) and Satake & Tanioka (2003) for the earthquake source (contours) and according to Watts *et al.* (2003) for the slide source (colour map). The solid and dashed contours indicate the initial coseismic seafloor uplift and subsidence, respectively. The grey circles show one-day aftershocks from USGS. (c) A 3-D view of the landslide source shown in panel (b). (d) Original tide gauge records of the tsunami. (e) The respective detided tsunami waveforms.

An analysis of hydroacoustic records, or T-phase, indicated that the slide/slump was generated at 9:02 GMT, 13 min after the main shock, which was also supported by eyewitness accounts of arrival time of the large waves (Okal 1999; Synolakis *et al.* 2002). The hydrophone records at Wake Island (see Fig. 1a for location), associated with an aftershock (M 4.4) at 9:02 GMT, showed unusually large amplitude and long duration compared to another aftershock, probably contributing to the tsunami generation by the submarine slump (Okal 1999; Synolakis *et al.* 2002). Except for the distribution of runup heights along the nearest coastline, no information has been available about the tsunami wave heights, wave periods and propagation properties in the near-field or middle range because no

tsunami waveforms were studied. Only far-field tide gauge records from Japan were reported in previous studies (Tanioka 1999; Satake & Tanioka 2003).

3 DATA AND METHODOLOGY

3.1 Data

Our data included four tide gauge records in Lombrum, Rabaul, Malakal Island and Yap Island with sampling intervals of 1 min, 15 s, 2 min and 2 min, respectively (see Figs 1a and 2 for locations and

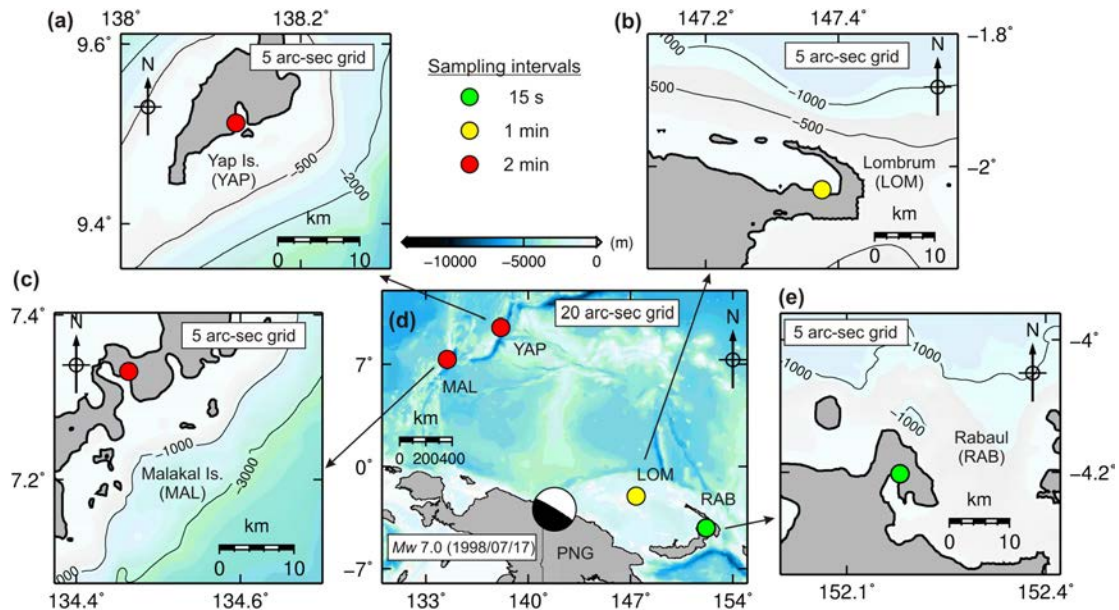


Figure 2. The bathymetry grids used for modelling the 1998 July 17 Papua New Guinea earthquake and tsunami. (a, b, c, e) The 5 arcsec bathymetric grid, interpolated from 30 arcsec GEBCO grid, around four tide gauge stations of Lombrum, Rabaul, Yap Island and Malakal Island. (d) The 20 arcsec bathymetric grid for the region. *LOM*, *RAB*, *MAL* and *YAP* represent Lombrum, Rabaul, Malakal Island and Yap Island, respectively.

Figs 1d–e for tsunami records). The data for Lombrum and Rabaul were supplied by the National Tidal Unit of the Australia Bureau of Meteorology and the Rabaul Volcanological Observatory (PNG), respectively. The data for Malakal and Yap Islands were provided by the Pacific Tsunami Warning Center of the U.S. National Oceanic and Atmospheric Administration. These four tide gauge records were the only ones that showed clear tsunami signals among around 50 tide gauge records investigated in the course of this study.

3.2 Tsunami waveform preparations

For tsunami waveform preparations, we applied the TASK tidal package (Tidal Analysis Software Kit, Bell *et al.* 2000) to estimate the tidal signal using harmonic analysis; then the tidal signals were removed from the original tide gauge records. High- and band-pass filters of Butterworth Infinite Impulse Response (IIR) digital filters (Mathworks 2014) were applied to decompose the records into high- and low-frequency components. The 5th order Butterworth digital filters were applied in this study.

3.3 Spectral analysis

Two types of spectral analyses were performed: Fourier and wavelet analyses. Fourier analysis was performed using Welch's averaged modified-periodogram method considering Hamming windows and overlaps for which we used the Matlab command *pwelch* (Mathworks 2014). In order to prevent reflected waves from appearing in the results of Fourier analysis, we used only the first 4-h segments of the tsunami waveforms after tsunami arrivals for performing Fourier analysis. A window length of 90 min was used for Hamming windowing of the tsunami waveforms with 30 per cent of overlaps between them.

The other spectral analysis, wavelet analysis, was performed using the well-tested wavelet package by Torrence & Compo (1998). Wavelet analysis reveals the frequency–time content of the tsunami waveforms and shows how tsunami spectral peaks change by pass-

ing time. Hence, it is also known as frequency–time analysis. For wavelet analysis, the *Morlet* mother function was used with a wavenumber of 6 and a wavelet scale width of 0.10.

3.4 Numerical modelling

Numerical modelling of tsunami was performed using the Cornell Multi-grid Coupled Tsunami Model (COMCOT) nonlinear shallow water (NSW) model (Liu *et al.* 1998) on a two-level nesting grids with spacing of 20 arcsec (Fig. 2d) and 5 arcsec (Figs 2a, b, c and e). All grids were resampled from the 30 arcsec GEBCO bathymetric grid (IOC *et al.* 2003). Simulations were performed using a time step of 0.5 s. Analytical formula by Okada (1985) were used to calculate the initial seafloor deformation due to the earthquake using the fault parameters of strike: 110° , dip: 20° , rake: 90° , length: 40 km, width: 20 km, top depth of the fault: 5 km and slip: 1.0 m (Synolakis *et al.* 2002; Satake & Tanioka 2003). For modelling the landslide/slump tsunami, the initial 3-D water surface at the end of slide/slump motion was estimated using semi empirical equations by Watts *et al.* (2005), and then was fed to the tsunami propagation model along with the initial velocities (Heidarzade & Satake 2014a). According to Watts *et al.* (2003), submarine slump source parameters were as length: 4.5 km, width: 5 km, water depth: 1500 m, thickness: 760 m, bulk density: 2150 kg m^{-3} and travel distance: 375 m.

4 STATISTICAL PROPERTIES

The tsunami was clearly recorded in all four stations (Figs 1d–e and 3a). In Rabaul, a long wave with period of ~ 30 min was observed before the tsunami arrival (Fig. 1e). Such a long wave with monochromatic oscillation is possibly a seiche mode of the region. This non-tsunami signal was removed from the record of Rabaul by high-pass filtering (Fig. 3a). To estimate the tsunami durations at tide gauge stations, we calculated the root mean square of the sea level data (Fig. 3b). The duration of tsunami oscillations was in the range of 8–10 h in different stations (grey-faced areas in Fig. 3b).

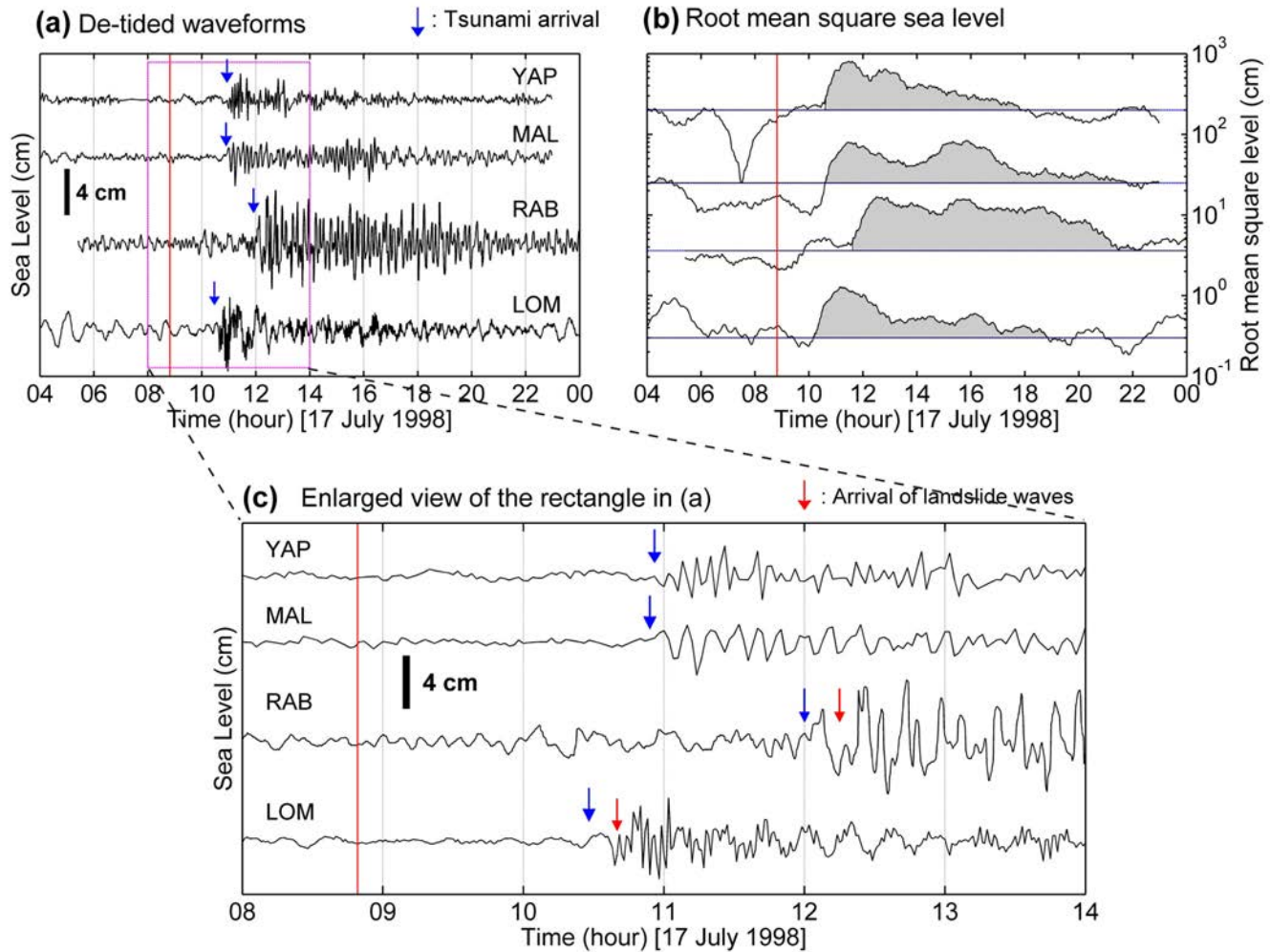


Figure 3. (a) Detided tsunami waveforms. The record of Rabaul (RAB) is high-pass filtered with a cut-off period of 27 min. (b) Root mean square of the tide gauge records. The grey-coloured areas show the duration times of tsunami oscillation. (c) Part of the de-tided waveforms in the time window shown by the purple rectangle in panel (a). LOM, RAB, MAL and YAP represent Lombrum, Rabaul, Malakal Island and Yap Island, respectively. The blue and red arrows show the arrival times of the first tsunami waves and the landslide-generated waves, respectively.

The recorded wave heights on the tide gauges, which range from 3 to 9 cm, are much smaller than the observed runup height of up to ~ 15 m on the nearest coast. This can be attributed to several factors: (1) the tide gauge stations are located at least 600 km away from the source, compared to the large runup heights recorded within 10 km of the source, (2) most stations are located inside confined bays which are sheltered from the incident tsunami waves (Fig. 2) and (3) most of the coastal runup heights of the PNG tsunami were attributed to the landslide-generated waves which usually lose their large amplitudes rapidly. Nevertheless, the instrumental tsunami waveform data provide us with important information about tsunami characteristics such as spectral properties and arrival times of the tsunami.

In all stations, the arrival times were not clear due to high noise levels and small tsunami amplitudes. However, the enlarged view of the tsunami waveforms (Fig. 3c) showed that the period of the first cycle of tsunami wave was noticeably longer than the following tsunami waves in Lombrum and Rabaul. This initial tsunami phase has a period of ~ 10 – 15 min followed by shorter waves with periods < 5 min (Fig. 3c). By assuming that the initial longer-period signals belong to the earthquake source of this tsunami and the later shorter-period signals belong to the landslide source, this observation is

possibly evidence for the reported delay in landslide generation (Synolakis *et al.* 2002). According to Fig. 3(c), the time delays in landslide generation were ~ 13 and ~ 15 min for the Lombrum and Rabaul tide gauge records, respectively. We further discuss this delay for landslide generation in the following sections.

5 SPECTRAL PROPERTIES

The spectra and spectral ratios are presented in Fig. 4. According to Fig. 4(left-hand column), most of the tsunami energy of the four tide gauge records is distributed in the period band of 1–20 min. For Lombrum (Fig. 4a), several peaks of the tsunami energy can be divided into two groups; one at 2–4 min (zone B) and another at 6–20 min (zone A) with a clear separation at period of ~ 5 min. Such two groups of peaks are not clear in other spectral plots because the sampling intervals and the distances from the tsunami source are different. To better distinguish tsunami signals from non-tsunami ones, we calculated spectral ratios which are the results of dividing the tsunami spectra by the background ones (Fig. 4, right-hand panel). Rabinovich (1997) showed that spectral ratio is a useful tool for identifying tsunami source signals because it shows large amplifications at periods belonging to the tsunami source. The separation

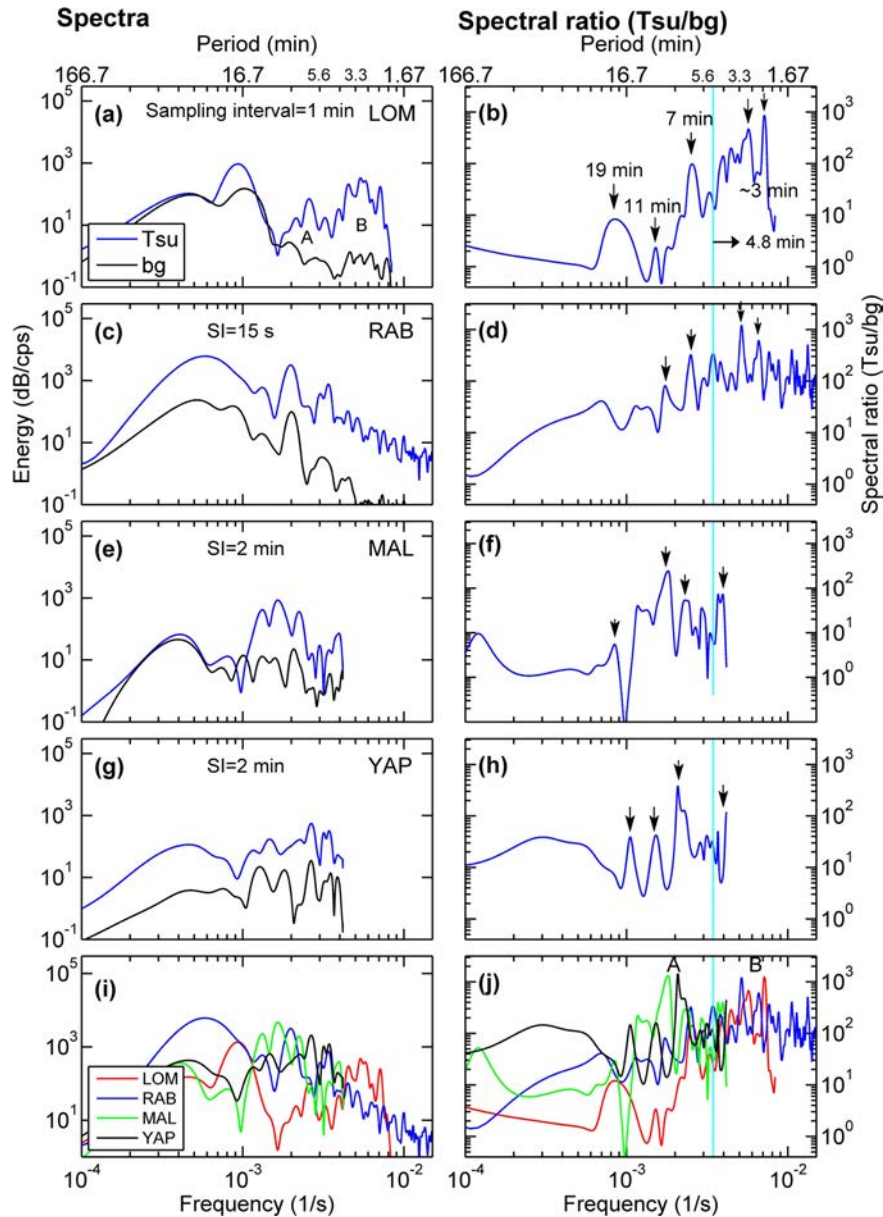


Figure 4. Spectra (left-hand panels; a, c, e, g, i) and spectral ratios (right-hand panels; b, d, f, h, j) for the tide gauge records of the 1998 July 17 Papua New Guinea Tsunami. *Tsu*, *bg* and *SI* represent tsunami, background and sampling intervals, respectively. The vertical-cyan lines in the right panels show the spectral trough at the period of 4.8 min between the two peak period-bands of 2–4 (zone B) and 6–20 min (zone A) which we attribute to the landslide and earthquake sources of this tsunami, respectively. *LOM*, *RAB*, *MAL* and *YAP* represent Lombrum, Rabaul, Malakal Island and Yap Island, respectively.

of two peak period bands, discussed above for the spectral peaks of the Lombrum record, can be seen more or less in spectral ratios of other stations (Fig. 4, right-hand panel). The overlaid spectral ratios from all four records is shown in Fig. 4(j) in which a clear spectral trough at period of around 5 min (the vertical cyan line) can be seen between the two peak period bands of 2–4 min (zone B) and 6–20 min (zone A). We attribute the aforesaid peak spectral bands to the landslide and earthquake sources of the 1998 PNG tsunami, respectively.

To further confirm this finding, we apply band-pass filtering to decompose the observed tide gauge records at Lombrum and Rabaul into two waveforms with periods <4 min and >4 min which might represent the landslide and earthquake sources of the 1998 PNG tsunami, respectively (Figs 5a and b). This analysis is not applicable to the records of Malakal and Yap Islands because the short-

est signal existing in their records is 4 min due to their sampling intervals of 2 min. According to Fig. 5(a), the largest wave amplitudes belong to the shorter-period waveform (periods <4 min) in Lombrum whereas most of the wave amplitudes are produced by the longer-period waveform (periods >4 min) in Rabaul (Fig. 5b). This may indicate that the landslide-generated waves were dominating in Lombrum whereas the earthquake-generated waves were dominating in Rabaul. This is possibly because the Rabaul station is located at ~1120 km from the source, twice farther compared to the Lombrum station which is located at ~600 km, and the landslide-generated waves lose their amplitudes rapidly.

The blue vertical lines in Figs 5(a) and (b) indicate time delays of ~12 and ~17 min between the arrival times of the landslide- and earthquake-generated waves for the Lombrum and Rabaul stations, respectively. These values for delays in landslide generation are

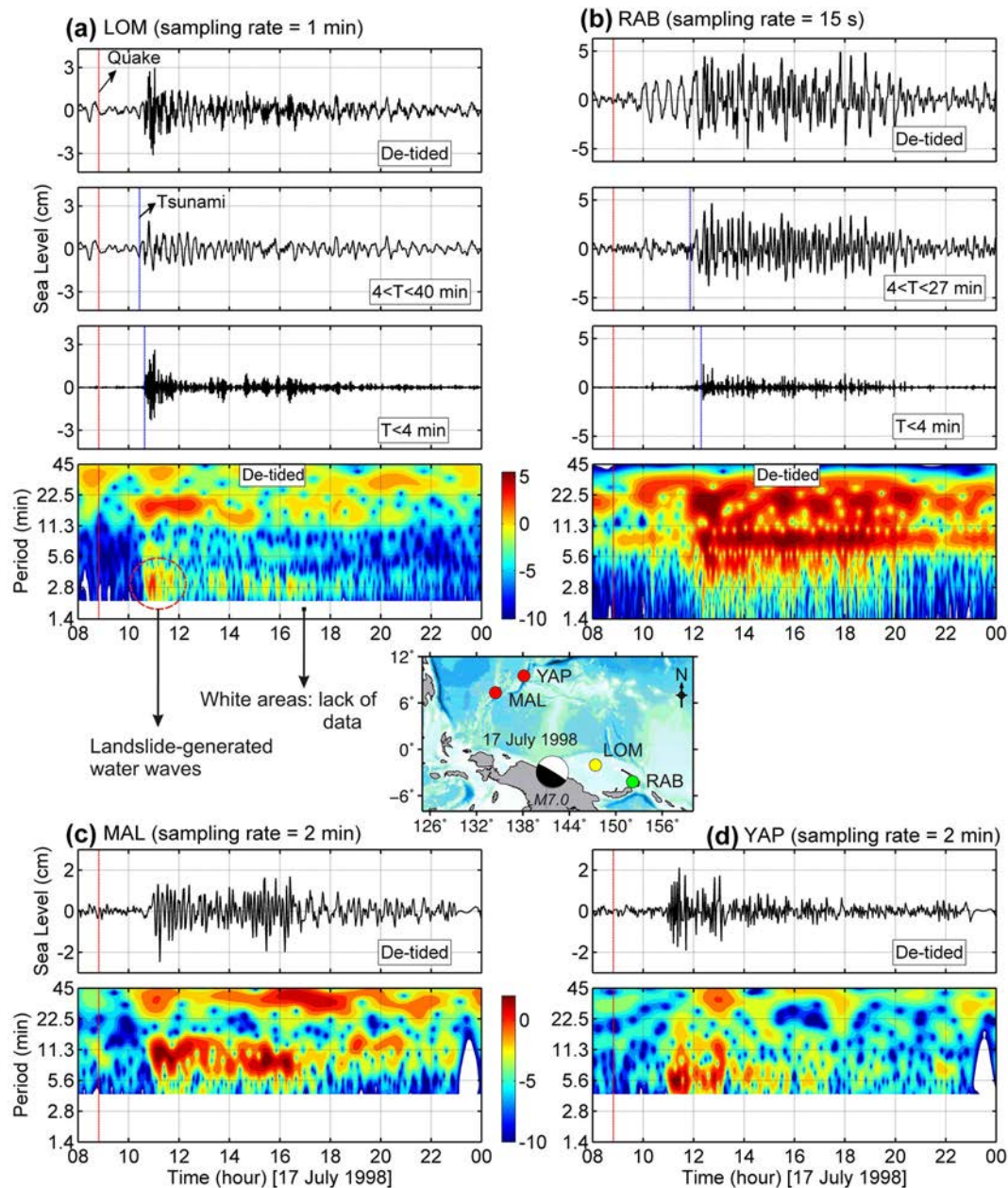


Figure 5. (a)–(b) Original detided records and decomposed waveforms at periods < 4 min and > 4 min along with wavelet plots for Lombrum and Rabaul stations. (c)–(d) Detided waveforms along with wavelet plots for the Malakal and Yap Islands. For all stations, the wavelet analysis is performed for the detided records. T stands for wave period. The white areas within the wavelet panels show areas without data because of the long sampling intervals. *LOM*, *RAB*, *MAL* and *YAP* represent Lombrum, Rabaul, Malakal Island and Yap Island, respectively.

close to those obtained in previous section (Fig. 3c). The wavelet plot for Lombrum clearly shows distinct patches of tsunami energy at the period band of 2–4 min which we attribute to the landslide source of this tsunami (dashed circle in Fig. 5a). Such patches were not observed at the 2–4 min band for Rabaul although we see some energy at this band (Fig. 5b).

The expected tsunami periods from the landslide and earthquake sources of the PNG tsunami can be roughly estimated using formulae $T = \frac{2L}{\sqrt{gd}}$, where T is tsunami period, L is source dimension, g is gravitational acceleration (9.81 m s^{-2}) and d is water depth at the source location (Rabinovich 2009; Heidarzadeh & Satake 2014b). By using the source dimensions of 40 and 20 km for earthquake source, a source dimension of 5–7 km for the landslide source, and

a water depth in the range 1000–2000 m, the resulting water wave periods are 1–2.5 min for the landslide source and 5–14 min for the earthquake source. These theoretical values are close to those obtained from our spectral analysis of the observed tide gauge records.

6 RESULTS OF NUMERICAL MODELLING

Our aims for conducting numerical simulations were: (1) to examine whether the available earthquake and landslide source models for the 1998 PNG tsunami (e.g. Tanioka 1999; Heinrich *et al.* 2000, 2001; Synolakis *et al.* 2002; Satake & Tanioka 2003; Watts *et al.* 2003) are consistent with the tide gauge records of this tsunami

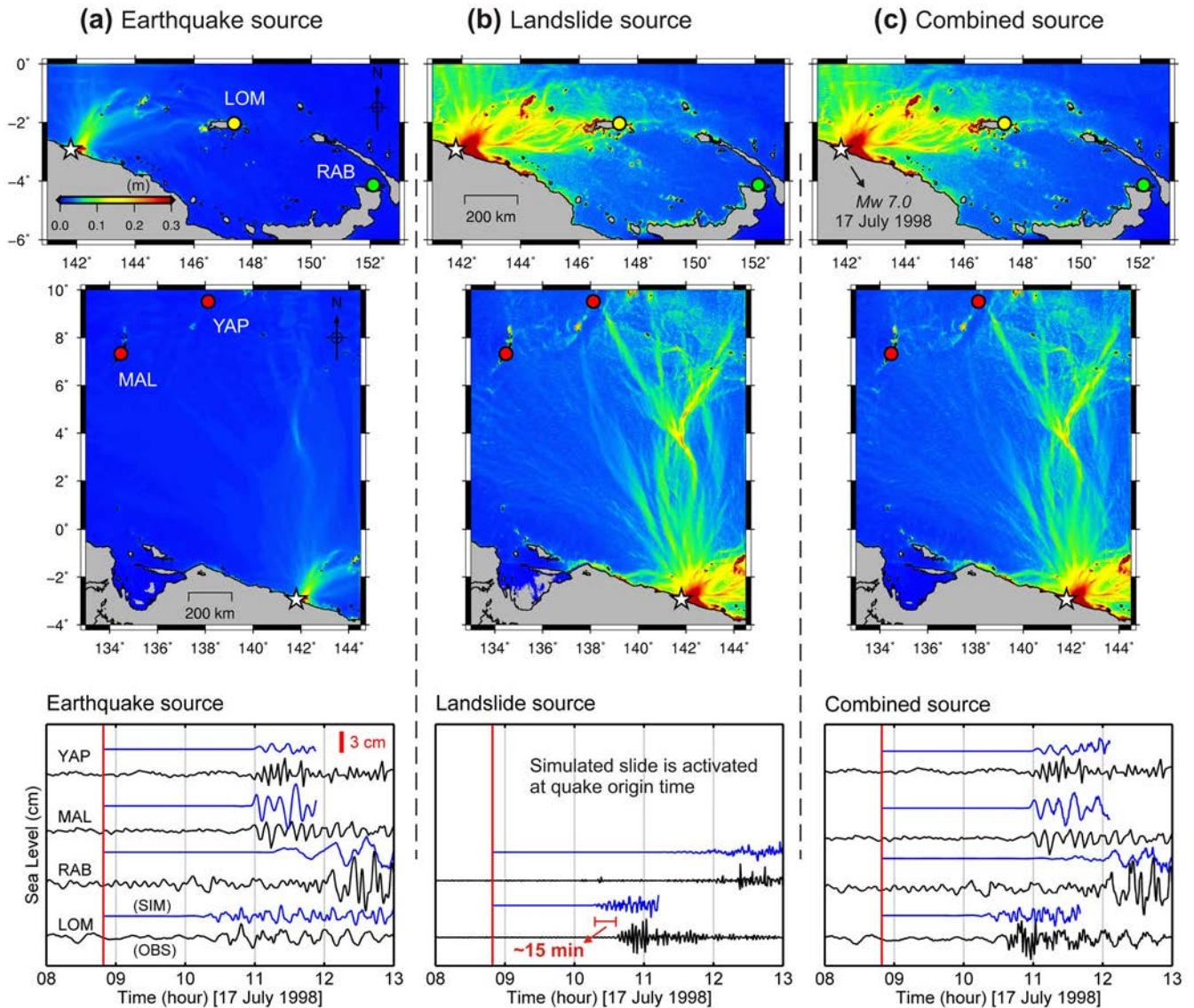


Figure 6. (a/top and middle) Distribution of maximum tsunami amplitudes from the earthquake source. (a/bottom) Comparison of the simulated and observed records. The observed waveforms here are the decomposed ones for the earthquake source; that is, waves with periods >4 min. (b) The same as (a) but for the landslide source. The landslide source here is activated at the earthquake origin time. The observed waveforms here are the decomposed ones for the landslide source; that is, waves with periods <4 min. (c) The same as (a) but for the combined source in which the earthquake source is launched at the origin time and then the landslide source is launched after 13 min. The observed waveforms here are the original detided ones. In all cases, the simulated waveforms at Lombrum, Rabaul, Malakal and Yap Islands were resampled at the sampling intervals of the observed records at these stations which are: 1, 0.25, 2 and 2 min, respectively. *LOM*, *RAB*, *MAL* and *YAP* represent Lombrum, Rabaul, Malakal Island and Yap Island, respectively.

or not and (2) to propose a combined source consisting of both earthquake and landslide sources for the PNG tsunami.

Fig. 6 presents the results of numerical modelling of tsunami propagation using the available source models proposed for the 1998 PNG tsunami. The simulations were performed using three different sources: (1) the earthquake source of the tsunami according to the source model proposed by Synolakis *et al.* (2002) and Satake & Tanioka (2003) (results in Fig. 6, left-hand panels), (2) the landslide source model according to Watts *et al.* (2003) (results in Fig. 6, middle panels) which was activated at earthquake origin time and (3) the combined source in which the landslide source was activated 13 min after the earthquake origin time (results in Fig. 6, right-hand panels). In Fig. 6, the simulation results from the landslide and earthquake sources are compared with the corresponding observation signals; that is, observed waveforms with periods

<4 min and >4 min for the landslide and earthquake sources, respectively. The simulated waveforms were also resampled at the sampling intervals of each tide gauge record so that the observed and simulated waveforms can be compared directly.

In all three cases, the simulated and observed waves fairly agree. For the landslide source (Fig. 6, middle panels), the simulated waves arrive ~ 15 min earlier than the observed ones. As the landslide source for this case was activated at the earthquake origin time, this is the other evidence showing that a time delay of ~ 15 min is necessary for landslide generation. For the combined source, the landslide source was activated 13 min after the earthquake origin time, as proposed by Okal (1999) and Synolakis *et al.* (2002). Both the arrival times and the amplitudes of the observed and simulated waves agree fairly well in the combined source (Fig. 6c). The simulated waveforms with the sampling intervals of 0.5 s are shown

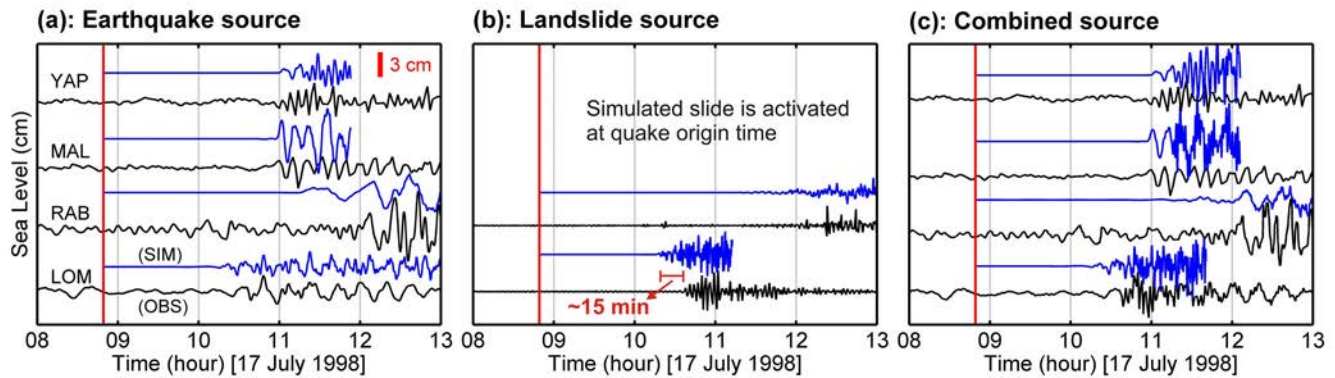


Figure 7. The same as Fig. 6 but sampling intervals for the simulated waveforms (blue waveforms) are 0.5 s. (a) Comparison of the simulated and observed records for the earthquake source. The observed waveforms here are the decomposed ones for the earthquake source; that is, waves with periods >4 min. (b) The same as (a) but for the landslide source. The landslide source here is activated at the earthquake origin time. The observed waveforms here are the decomposed ones for the landslide source; that is, waves with periods <4 min. (c) The same as (a) but for the combined source in which the earthquake source is launched at the origin time and then the landslide source is launched after 13 min. The observed waveforms here are the original de-tided ones.

in Fig. 7 indicating that the simulated amplitudes are larger than the observed ones at Malakal and Yap Islands. Since the sampling intervals of the observed records at these two stations were 2 min, the waves with periods <4 min were not recorded at these two stations. In other words, the landslide-generated waves were not possibly recorded in Malakal and Yap Islands, hence the observed waveforms lack the contribution from the landslide source.

Distribution of the maximum tsunami amplitudes (Fig. 6, top and middle rows) indicates that the landslide source is governing the tsunami wave field in the computational domain. While most of the tsunami amplitude is directed normal to the fault strike for the earthquake source (Fig. 6, left-hand panel), the tsunami energy is directed in almost all directions for the landslide source at distances <200 km (Fig. 6, middle panel). In addition, it is clear that a large part of the tsunami amplitude moves along the shallow waters to the north and east of the source region. In particular, beams of large tsunami amplitudes are directed towards Lombrum and Yap Island. For Lombrum, such a beam is larger for the landslide source compared to the earthquake one which may explain the observed large wave amplitudes from the former source in this station.

In summary, results of numerical modelling may indicate that the available source models for the 1998 PNG tsunami (both landslide and earthquake sources) are fairly consistent with the tide gauge records although those source models were not validated with these tide gauge records in the past. A combined source model in which the landslide source is activated 13 min after the earthquake source is compatible with the observed four tide gauge records both in terms of tsunami amplitudes and arrival times.

7 CONCLUSIONS

The 1998 July 17 Papua New Guinea tsunami has been studied using newly retrieved tide gauge records in Lombrum, Rabaul, Malakal Island and Yap Island. Main findings are:

- (1) The 1998 PNG tsunami produced a trough-to-crest wave height of 3–9 cm at tide gauges located 600–1450 km away from the source.
- (2) Analysis of the tsunami waveforms revealed 12–17 min delay in landslide generation compared to the origin time of the main shock. This is the first direct evidence of delayed landslide source of the PNG tsunami which was previously indirectly estimated from acoustic T-phase records.

- (3) The landslide and earthquake source period bands of the tsunami were 2–4 min and 6–20 min, respectively.

(4) We quantitatively studied the contribution of landslide and earthquake sources to the 1998 PNG tsunami by analysing tide gauge records.

(5) Our numerical modelling showed that a combined source model consisting of a landslide source activated 13 min after the earthquake source, reproduced fairly well the observed tide gauge records of the 1998 PNG tsunami.

ACKNOWLEDGEMENTS

The tide gauge records used in this study were provided by the National Tidal Unit of the Australia Bureau of Meteorology, the Rabaul Volcanological Observatory and the Pacific Tsunami Warning Center of the U.S. National Oceanic and Atmospheric Administration (NOAA). Some Figures were drafted using the GMT software (Wessel & Smith 1991). We sincerely thank Stuart Weinstein from NOAA for providing the tide gauge records of Malakal and Yap Islands. We thank Takeo Ishibe, Tomoya Harada, Aditya Gusman and Dun Wang (all from ERI, Tokyo University) for commenting on an early version of the manuscript. This study was supported by the Japan Society for the Promotion of Science (JSPS) grant number JSPS/FF1/202.

REFERENCES

- Bell, C., Vassie, J.M. & Woodworth, P.L., 2000. POL/PSMSL Tidal Analysis Software Kit 2000 (TASK-2000), Permanent Service for Mean Sea Level, CCMS Proudman Oceanographic Laboratory, UK.
- Geist, E.L., 2000. Origin of the 17 July 1998 Papua New Guinea tsunami: earthquake or landslide, *Seismol. Res. Lett.*, **71**(3), 344–351.
- Heidarzadeh, M. & Satake, K., 2014a. Possible sources of the tsunami observed in the northwestern Indian Ocean following the 2013 September 24 Mw 7.7 Pakistan inland earthquake, *Geophys. J. Int.*, **199**(2), 752–766.
- Heidarzadeh, M. & Satake, K., 2014b. New insights into the source of the Makran Tsunami of 27 November 1945 from Tsunami waveforms and coastal deformation data, *Pure appl. Geophys.*, **172**(3–4), 621–640.
- Heinrich, P., Piatanesi, A., Okal, E. & Hébert, H., 2000. Near-field modeling of the July 17, 1998 tsunami in Papua New Guinea, *Geophys. Res. Lett.*, **27**(19), 3037–3040.
- Heinrich, P., Piatanesi, A. & Hébert, H., 2001. Numerical modelling of tsunami generation and propagation from submarine slumps: the 1998 Papua New Guinea event, *Geophys. J. Int.*, **145**(1), 97–111.

- IOC, IHO & BODC, 2003. Centenary edition of the GEBCO digital atlas, published on CD-ROM on behalf of the Intergovernmental Oceanographic Commission and the International Hydrographic Organization as part of the general bathymetric chart of the oceans, British oceanographic data centre, Liverpool, UK.
- Kikuchi, M., Yamanaka, Y., Abe, K. & Morita, Y., 1999. Source rupture process of the Papua New Guinea earthquake of July 17, 1998 inferred from teleseismic body waves, *Earth Planets Space*, **51**(12), 1319–1324.
- Liu, P.L.-F., Woo, S.-B. & Cho, Y.-S., 1998. Computer programs for tsunami propagation and inundation, Technical report, Cornell University, 111 pp.
- Lynett, P.J., Borrero, J.C., Liu, P.L.-F. & Synolakis, C.E., 2003. Field survey and numerical simulations: a review of the 1998 Papua New Guinea tsunami, *Pure appl. Geophys.*, **160**, 2119–2146.
- Mathworks, 2014. MATLAB User Manual, The Math Works Inc., MA, USA, 282 pp.
- Matsuyama, M., Walsh, J.P. & Yeh, H., 1999. The effect of bathymetry on tsunami characteristics at Sisano Lagoon, Papua New Guinea, *Geophys. Res. Lett.*, **26**(23), 3513–3516.
- McSaveney, M.J., Goff, J.R., Darby, D.J., Goldsmith, P., Barnett, A., Elliott, S. & Nongkas, M., 2000. The 17 July 1998 tsunami, Papua New Guinea: evidence and initial interpretation, *Mar. Geol.*, **170**(1), 81–92.
- Okada, Y., 1985. Surface deformation due to shear and tensile faults in a half-space, *Bull. seism. Soc. Am.*, **75**(4), 1135–1154.
- Okal, E.A., 1999. The 1998 Papua New Guinea tsunami: an overview, in *Proceedings of the Intl. Conf. Tsunamis*, Paris, France, 26–28 May, pp. 111–116.
- Okal, E.A. & Synolakis, C.E., 2004. Source discriminants for near-field tsunamis, *Geophys. J. Int.*, **158**(3), 899–912.
- Rabinovich, A.B., 1997. Spectral analysis of tsunami waves: separation of source and topography, *J. geophys. Res.*, **102**(12), 663–676.
- Rabinovich, A.B., 2009. Seiches and harbour oscillations, in *Handbook of Coastal and Ocean Engineering*, World Scientific Publishing Company, pp. 193–236.
- Satake, K. & Tanioka, Y., 2003. The July 1998 Papua New Guinea earthquake: mechanism and quantification of unusual tsunami generation, *Pure appl. Geophys.*, **160**(10–11), 2087–2118.
- Synolakis, C.E., Bardet, J.-P., Borrero, J.C., Davies, H.L., Okal, E.A., Silver, E.A., Sweet, S. & Tappin, D.R., 2002. The slump origin of the 1998 Papua New Guinea tsunami, *Proc. R. Soc. Lond., A*, **458**(2020), 763–789.
- Tanioka, Y., 1999. Analysis of the far-field tsunamis generated by the 1998 Papua New Guinea Earthquake, *Geophys. Res. Lett.*, **26**(22), 3393–3396.
- Tappin, D.R., Matsumoto, T., Watts, P., Satake, K., McMurtry, G.M., Matsuyama, M. & Lafoy, Y., 1999. Sediment slump likely caused 1998 Papua New Guinea tsunami, *EOS, Trans. Am. geophys. Un.*, **80**(30), 329–340.
- Tappin, D.R., Watts, P., McMurtry, G.M., Lafoy, Y. & Matsumoto, T., 2001. The Sissano, Papua New Guinea tsunami of July 1998—offshore evidence on the source mechanism, *Mar. Geol.*, **175**(1), 1–23.
- Torrence, C. & Compo, G., 1998. A practical guide to wavelet analysis, *Bull. Am. Met. Soc.*, **79**, 61–78.
- Watts, P., Grilli, S.T., Kirby, J.T., Fryer, G.J. & Tappin, D.R., 2003. Landslide tsunami case studies using a Boussinesq model and a fully nonlinear tsunami generation model, *Nat. Hazards Earth Sys. Sci.*, **3**(5), 391–402.
- Watts, P., Grilli, S.T., Tappin, D. & Fryer, G.J., 2005. Tsunami generation by submarine mass failure. II: predictive equations and case studies, *J. Waterway Port Coastal Ocean Eng.*, **131**(6), 298–310.
- Wessel, P. & Smith, W.H.F., 1991. Free software helps map and display data, *EOS, Trans. Am. geophys. Un.*, **72**, 441.